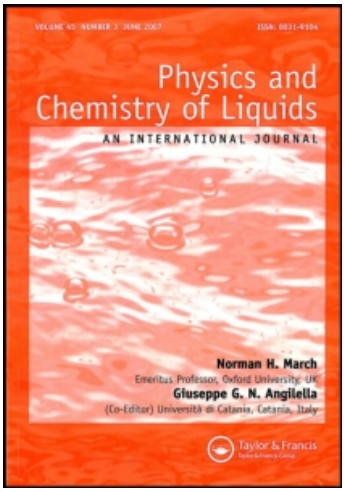

Physics and Chemistry of Liquids
Publication details, including instructions for authors and subscription information:
http://www.informaworld.com/smpp/title~content=t713646857

Interatomic Core Forces Deduced From Observed Liquid Structure Factors

A. Meyer[a]; M. Silbert[b]; W. H. Young[b]
[a] Department of Physics, Northern Illinois University, DeKalb, IL, USA [b] School of Mathematics and Physics, University of East Anglia, Norwich, UK

To cite this Article Meyer, A. , Silbert, M. and Young, W. H.(1984) 'Interatomic Core Forces Deduced From Observed Liquid Structure Factors', Physics and Chemistry of Liquids, 13: 4, 293 — 311
To link to this Article: DOI: 10.1080/00319108408080788
URL: http://dx.doi.org/10.1080/00319108408080788

Phys. Chem. Liq., 1984, Vol. 13, pp. 293–312
0031-9104/84/1304-0293$18.50/0

Printed in the United Kingdom

Interatomic Core Forces Deduced From Observed Liquid Structure Factors

A. MEYER,

Department of Physics, Northern Illinois University, DeKalb, IL 60115, USA

and

M. SILBERT and W. H. YOUNG

School of Mathematics and Physics, University of East Anglia, Norwich, UK

(*Received September 19, 1983*)

A simplified version of the WCA theory allows us to start from an observed structure factor and derive a core potential and gradient at an effective collision diameter. The quality of fit and internal consistency checks indicate that the method works for liquids of inert gases, certain simple metals and the noble metals. It is less accurate, although still useful, for transition metals and lanthanides. In the latter case, there is a peaking in core diameter at Eu($4f^7 6s^2$) as the series is traversed. This has no counterpart in the transition metal series which shows a steady decrease (although with an anomalously small value for Cr($3d^5 4s^1$)).

I INTRODUCTION

The aim of the present work is to interpret observed liquid structure factors at large momentum transfer (for a few oscillations beyond the principal peak). This region is expected to be described by the core only of the interatomic potential and this in turn is roughly characterised by hard sphere interactions.[1] But the latter is not a quantitative description and Weeks *et al.*[2] have proposed a formalism based on softened hard spheres which has been shown to be accurate[3] for a number of test cases when compared with molecular dynamic and Monte Carlo results.

In this WCA method, a core potential is specified and a structure factor is calculated. This raises the question of whether the inverse process can be achieved. The present authors[4] have argued that on the basis of the available

experimental evidence the structure factor in this region of interest appears to be decided by little more than the value of the potential gradient at some effective collision diameter.

To make this point explicitly, we used[4] a linearized version of the WCA and, in the following, we exploit this formalism by showing that in suitable[5] cases we can work back from an observed structure factor to the limited information indicated above.[6] After the method is explained (Section II), we turn to an examination of the results in the subsequent sections. Some general comments are made in Section III and these are followed with detailed scrutinies in turn of the results for the rare gas liquids (Section IV), the simple metals (Section V), the noble metals (Section VI), the transition metals (Section VII) and the lanthanides (Section VIII).

The method also contains some internal consistency tests which enable us to assess the validity of the present procedure in most cases. On this basis we are able to make some appraisal of the quality of the deduced data. These matters are discussed throughout the paper but are finally reviewed in Section IX.

II THEORY

The WCA method applies to fluids the atoms of which interact by pairwise forces of such a type that, in leading order, only the cores contribute to the free energy and structure factor (at large arguments). The idea is to approximate the latter quantities by those of a suitable hard sphere reference system and then apply corrections to incorporate core softening. This softening is described by a 'blip' function $B(r)$ which reflects the degree of departure of the true core potential, $u(r)$ say, from hard sphere form.

The 'best' hard sphere system is specified by diameter σ such that the blip function vanishes on average. In terms of the Fourier transform $\tilde{B}(k)$ this means

$$\tilde{B}(0) = 0 \tag{1}$$

This choice is most advantageous for the convergence of the free energy perturbation series. Since Eq. (1) recognizes $u(r)$ in only an average way, the method applies only to smooth cores which should also be steep in view of the perturbative character of the procedure.

The complete definition of the blip function is not necessary for present purposes. It suffices to say that the conditions of the previous paragraph ensure that it is highly localized about $r = \sigma$ in the form of two adjacent sharp 'teeth' one pointing upwards and one downwards. By approximating

these (or rather those for $r^2B(r)$) by triangles, Eq. (1) becomes[4,6]

$$U = \frac{-\beta\sigma u'(\sigma) + Y + 2}{-2\beta\sigma u'(\sigma) + Y + 2} \tag{2}$$

where $\beta = (k_B T)^{-1}$, $U = \exp\{-\beta u(\sigma)\}$ and $Y = \{d \ln g_\sigma(r)/d \ln r\}_{r=\sigma+0}$, $g_\sigma(r)$ being the radial distribution function of the hard sphere system.

When σ is thus prescribed, $r^2B(r)$ can be approximated[4,6] by the derivative of a Dirac delta function of suitable strength so that

$$n\tilde{B}(k) = A\left\{\left(\frac{\sin k\sigma}{k\sigma}\right) - \cos k\sigma\right\} \tag{3}$$

where

$$A = \frac{\mu(U - \frac{1}{2})^2}{U(1 - U)} \tag{4}$$

Here $\mu = 16\eta g_\sigma(\sigma + 0)/(Y + 2)^2$ and η is the hard sphere packing fraction given, for number density n, by $\eta = (\pi/6)n\sigma^3$.

To describe the structure factor $a(k)$ of the softened spheres, we need that of the hard spheres $a_\sigma(k)$ and the blip function. Then we use

$$a(k) = \frac{a_\sigma(k)}{\{1 - n\tilde{B}(k)a_\sigma(k)\}} \tag{5}$$

which is an improved version, derived by Jacobs and Andersen,[7] of the original WCA formula.

The hard sphere functions required above are analytically available[8] in Percus–Yevick approximation and are of tolerable accuracy but we have, in the present work, used the essentially exact formulae of Verlet and Weis.[9] Thus, for a given system (with specified $u(r)$) we can find σ from Eq. (2), then $\tilde{B}(k)$ from Eq. (3) and thence $a(k)$ from Eq. (5). In the end, the latter is characterized by only two independent parameters, σ, $u(\sigma)$ and $u'(\sigma)$ being connected by Eq. (2). For a truncated Lennard–Jones system, the approximations involved in deriving Eqs (2) and (3) (our simplified version of WCA theory) can be demonstrated explicitly[4] to be small and less than the effects obtained by changing to the Jacobs and Andersen form (5) from the original WCA expression.

In this paper, we are interested exclusively in the reverse procedure of matching Eq. (5) to experiment and extracting σ, $u(\sigma)$ and $u'(\sigma)$. Matching can never, of course, be perfect and the manner of 'best' fitting is to a certain extent arbitrary. However, once such a fitting has been made, the above formalism (as distinct from the full WCA counterpart) lends itself easily to the unique processing of the resulting information.

In practice, we chose σ and A in Eq. (5) so as to minimize

$$\int_{k_1}^{k_5} (a_{\text{expt}} - a)^2 k^2 dk,$$

where k_1 and k_5 correspond to the first and fifth nodes of $a(k) - 1$ beyond the principal peak. This takes advantage of the experience gained by Jacobs and Andersen who found that the WCA method works best at high k and is often very good around the third peak. With the optimum σ and A, Eq. (4) gives

$$U = \tfrac{1}{2}\{1 - [1 + (\mu/A)]^{-1/2}\} \tag{6}$$

and then, by Eq. (2),

$$\beta\sigma u'(\sigma) = \tfrac{1}{2}(Y + 2)\{[1 + (\mu/A)]^{1/2} + 1\} \tag{7}$$

III RESULTS; GENERAL COMMENTS

By the above method, we establish the data of Table I and these are the basis of all our subsequent discussion. We will consider the various categories in turn but a few rather general remarks will be made at once in the present section.

First, we comment upon the packing fraction sizes. It is often stated that liquids, at their triple points, having packing fractions of about 0.45–0.46. In a sense[12] this can be regarded as a consequence of variationally determining (by the Gibbs–Bogoliubov method) a best hard sphere system; hard spheres constitute the reference system and there is no attempt to improve upon that description. In the WCA procedure, the hard spheres are softened and, to allow for this, we must expect the diameters to be a little larger than those of the variational method. This is the origin of the packings, usually ~ 0.5 at the triple points, recorded in Table I.

The qualitative correspondence[1] between experiment and theory based on hard spheres is achieved, of course, by setting $A = 0$ in Eq. (3) and therefore $\tilde{B}(k) = 0$ in Eq. (5). This means, by Eq. (6), that $u(\sigma)/k_B T$ is always greater than $\ln 2 = 0.693$ and, in practice, for steep cores, should be somewhere near unity. It surprised us, however, to see the factors conspire in such a way as to make this ratio almost precisely unity for very many cases at melting. The results are shown in Table II; only in the case of Pb is the deviation as much as 10% and even here the deviation is smaller if we use data from other sources.[6] Above the melting temperatures, $u(\sigma)/k_B T$ decreases in all cases.

Ashcroft and Langreth[12] proposed that $u(\sigma)/k_B T \sim \frac{3}{2}$ while Silbert and Young[13] showed that the Gibbs–Bogoliubov method suggested a somewhat smaller value than this (between 1 and $\frac{3}{2}$). The present analysis suggests that

TABLE I

Analysis of observed structure factors; data summary

	Input		Output				
Atom	T/K	n/Å^{-3}	A	η	σ/Å	$u(\sigma)$/ev	$-\sigma u'(\sigma)$/ev
Ar	85	0.0213	0.0529	0.492	3.535	0.00675	0.1312
Ne	35	0.0317	0.0468	0.402	2.894	0.00248	0.0387
	35	0.0334	0.0564	0.426	2.900	0.00260	0.0396
	35	0.0347	0.0689	0.445	2.904	0.00272	0.0395
Li	463	0.0444	0.1044	0.501	2.782	0.0412	0.5769
Na	373	0.0243	0.1090	0.513	3.429	0.0341	0.4854
K	343	0.0127	0.1134	0.512	4.252	0.0315	0.4387
Rb	313	0.0104	0.1110	0.512	4.547	0.0286	0.4028
Cs	303	0.00833	0.1023	0.493	4.834	0.0266	0.3657
Mg	953	0.0383	0.0877	0.509	2.938	0.0832	1.312
Al	943	0.0528	0.0710	0.504	2.632	0.0790	1.374
	1023	0.0525	0.0798	0.486	2.606	0.0855	1.315
	1323	0.0507	0.0825	0.445	2.560	0.1053	1.391
Pb	613	0.0310	0.0389	0.482	3.096	0.0463	1.027
	823	0.0302	0.0462	0.453	3.060	0.0617	1.138
	1023	0.0295	0.0396	0.422	3.011	0.0732	1.321
	1173	0.0287	0.0459	0.402	2.991	0.0833	1.310
Cu	1423	0.0755	0.0797	0.526	2.369	0.1247	2.196
	1573	0.0745	0.0926	0.508	2.353	0.1385	2.117
	1773	0.0728	0.0876	0.484	2.333	0.1498	2.174
	1873	0.0722	0.0883	0.466	2.310	0.1548	2.108#
Ag	1273	0.0518	0.0944	0.514	2.667	0.1133	1.750
	1423	0.0509	0.0993	0.494	2.647	0.1245	1.751
	1573	0.0501	0.1009	0.478	2.631	0.1349	1.781
	1673	0.0496	0.0918	0.454	2.595	0.1367	1.753#
Au	1423	0.0526	0.0830	0.510	2.646	0.1233	2.012
	1573	0.0523	0.0921	0.500	2.634	0.1369	2.045
	1773	0.0517	0.0913	0.480	2.608	0.1500	2.101
	1973	0.0514	0.0881	0.448	2.555	0.1592	2.053#
V	2173	0.0634	0.1139	0.509	2.484	0.1989	2.732
Cr	2173	0.0726	0.0808	0.498	2.358	0.1847	2.939
Mn	1533	0.0655	0.0825	0.490	2.426	0.1293	1.978
Fe	1833	0.0756	0.0898	0.517	2.355	0.1624	2.603
Co	1823	0.0786	0.0999	0.498	2.296	0.1605	2.278
Ni	1773	0.0792	0.0952	0.489	2.276	0.1530	2.162
La	1243	0.0258	0.1133	0.440	3.195	0.1029	1.131
Ce	1143	0.0287	0.1135	0.437	3.077	0.0941	1.024
Pr	1223	0.0283	0.1190	0.451	3.124	0.1036	1.148
Nd	1323	0.0289	0.1257	0.458	3.117	0.1144	1.260
Eu	1103	0.0183	0.1048	0.413	3.507	0.0866	0.910
Gd	1603	0.0265	0.1322	0.474	3.246	0.1433	1.615
Tb	1653	0.0274	0.1252	0.473	3.204	0.1460	1.688
Dy	1703	0.0302	0.1284	0.478	3.117	0.1524	1.771
Ho	1753	0.0301	0.1359	0.458	3.073	0.1535	1.619
Er	1793	0.0301	0.1571	0.468	3.095	0.1638	1.651
Yb	1123	0.0216	0.0985	0.467	3.459	0.0946	1.222
Lu	1953	0.0316	0.1513	0.472	3.055	0.1783	1.855

Observed structure factors are from Yarnell *et al.*[10] (for Ar), de Graaf and Mozer[11] (for Ne) and Waseda[1] (all other cases). The Ne densities quoted correspond to pressures of 2.17, 8.00 and 14.18 MPa; all other cases are for 1 atm pressure, the first of each type quoted being for a temperature close to melting. The markers (#) indicate that we believe (see text) that these results are less accurate.

TABLE II

$u(\sigma)/k_B T$ near melting (1 atm) for the liquids of Table I

Ar	Li	Na	K	Rb	Cs	Mg	Al	Pb	Cu
0.92	1.03	1.06	1.07	1.06	1.02	1.01	0.97	0.88	1.02
Ag	Au	V	Cr	Mn	Fe	Co	Ni	La	Ce
1.03	1.01	1.06	0.99	0.98	1.03	1.02	1.00	0.96	0.96
Pr	Nd	Eu	Gd	Tb	Dy	Ho	Er	Yb	Lu
0.98	1.00	0.91	1.04	1.03	1.04	1.02	1.06	0.98	1.06

a useful criterion within the WCA framework is $u(\sigma)/k_B T \sim 1$. This is, of course, a more quantitative way of indicating that, under fixed conditions, WCA diameters are bigger than the corresponding Gibbs–Bogoliubov ones.

An index of core hardness can be extracted from the data by assuming that around $r = \sigma$ we have

$$u(\sigma)/k_B T \propto (\sigma/r)^n \tag{8}$$

In that case (Table II), the proportionality constant is almost unity and

$$n = -\sigma u'(\sigma)/u(\sigma) \tag{9}$$

The latter is tabulated in Table III for the liquids of Table I near melting (1 atm).

To understand the general size of these numbers, it is useful to note that the truncated Lennard-Jones potential $4\varepsilon[(\sigma_0/r)^6 - \frac{1}{2}]^2$ corresponds to an n of $12/[1 - \frac{1}{2}(\sigma/\sigma_0)^6]$. The latter tends to 12 as σ tends to zero but at more realistic values, say when $\sigma \simeq \sigma_0$, we obtain $n \simeq 24$. The result for *Ar* is entirely compatible with this argument and all the other (metallic) cases considered are softer (according to this definition) with the possible exception of Pb. It is worth mentioning, however, that if we were to use the data of other authors than Waseda for this case a marginally reduced value (comparable with that for Ar) would be obtained.[6]

We now examine individually the various classes of fluids.

TABLE III

$-\sigma u'(\sigma)/u(\sigma)$ near melting (1 atm) for the liquids of Table I

Ar	Li	Na	K	Rb	Cs	Mg	Al	Pb	Cu
19.4	14.0	14.2	13.9	14.1	13.8	15.8	17.4	22.2	17.6
Ag	An	V	Cr	Mn	Fe	Co	Ni	La	Ce
15.4	16.3	13.7	15.9	15.3	16.0	14.2	14.1	11.0	10.9
Pr	Nd	Eu	Gd	Tb	Dy	Ho	Er	Yb	Lu
11.1	11.0	10.5	11.3	11.6	11.6	10.6	10.1	12.9	10.4

IV INERT GAS LIQUIDS

In these cases, the method is very successful as might be expected since the WCA method was designed with such fluids in mind. A typical fit to experiment of a theoretical structure factor, as given by Eq. (4), is shown in Figure 1. As one must expect (Sections I, II), the theory fails at small k, but, in fact,

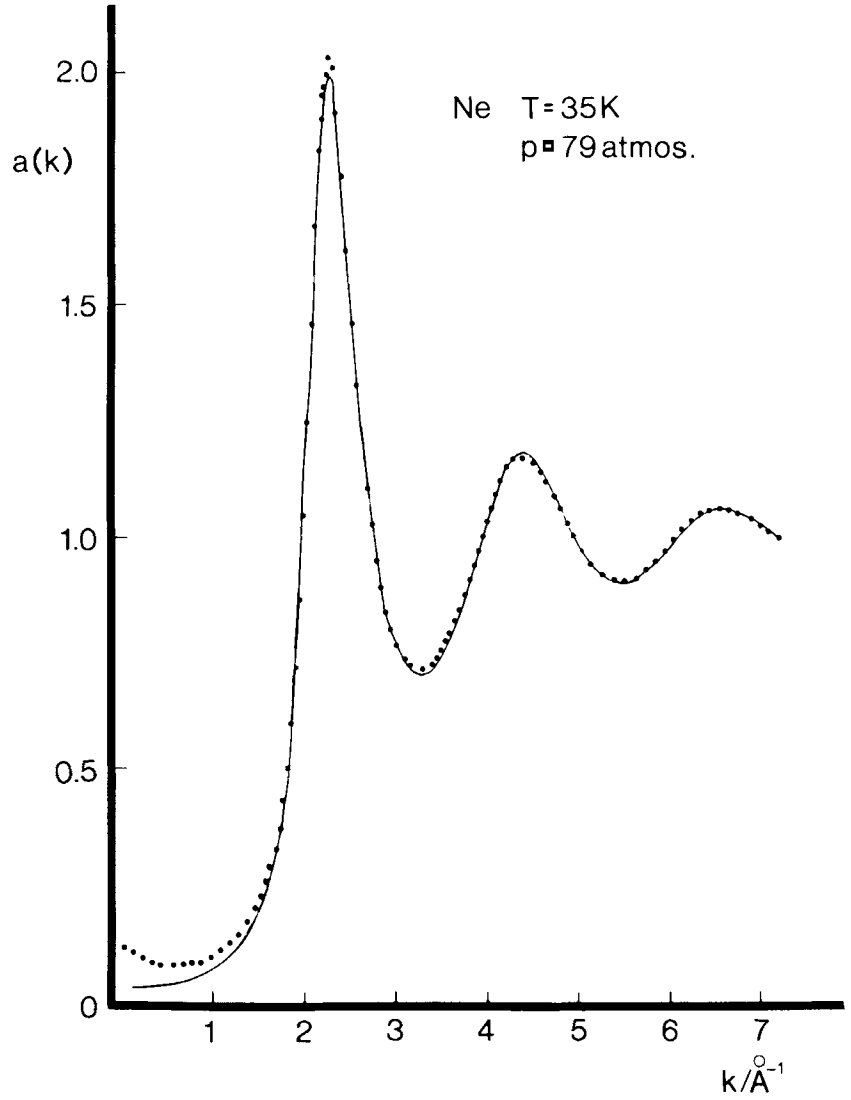

FIGURE 1 Structure factors for liquid Ne at 35 K and 8.00 MPa ($n = 0.0334$ Å^{-3}). The dots refer to experiment, the continuous lines to theory (Eq. (14) with A, σ given in Table I).

it works well around the principal peak even though this region plays no part in our optimizing process (Section II).

It will be seen from Table I that though the density of Ne is varied quite considerably, the parameters σ, $u(\sigma)$ and $u'(\sigma)$ hardly change. Crudely speaking, as compression occurs, the cores maintain their size while the interstitial space is reduced.

This insensitivity to pressure contrasts with the effect of the thermally induced density variations considered in subsequent sections; in the latter cases the temperature strongly affects the binary collision energy with a consequent strong variation in the parameters.

V SIMPLE METALS

Many of the simple metals have anomalous principal peaks[1] (skew or with shoulders) and some explanations of these[5] involve cores which are not amenable to WCA analysis. We confined our studies to cases where it seemed likely (from ab initio electron theory and the absence of anomalies of the above type) that the core potential rises smoothly as atoms approach each other closely. Such cases are the alkalis, Mg, Al and Pb.

As Jacobs and Andersen recognized, the alkali cores are too soft for truly successful fits to be made; there is always a phase difference at high k between corresponding experimental and theoretical curves.[14] Nevertheless, the fitted parameters are of at least qualitative interest in relation to those of the other systems investigated and we therefore quote them for completeness (Figure 2 and Table I).

The fits for Mg, Al and Pb are all satisfactory. Indeed that for Pb is remarkable in that matching of theory to experiment takes place down to very low k, much as for Ne in Figure 1. One such comparison for this metal has already been published[6] so we give here, in Figure 3, an example for the case of Al.

An internal consistency check can be made when the analysis has been performed for a given liquid at a number of temperatures. The point is illustrated in Figure 4 for Al where we use the data of Table I to plot $u(\sigma)$ versus σ and thereby begin to map out an interatomic core potential.[15] Furthermore, tangents are also available from the $u'(\sigma)$ of Table I and these are inserted in the figure in the form of short straight lines. The slopes of the latter should be consistent with each other and with the trend of the points mapping out $u(\sigma)$ versus σ. A good measure of consistency is, in fact, obtained; we attribute such imperfections as are to be seen in Figure 4 largely to experimental error. A similar analysis of the four sets of results given for Pb show them all to be consistent in the above sense.

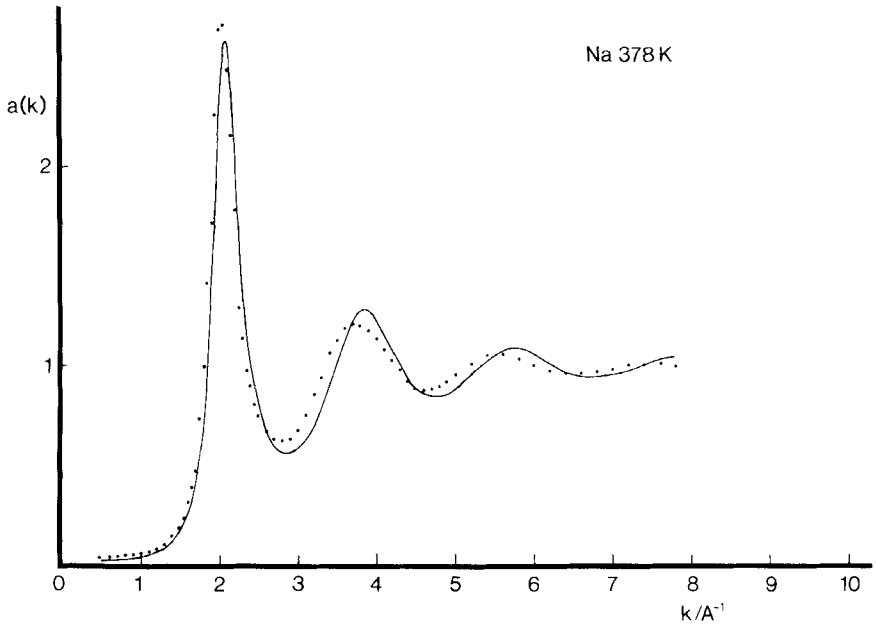

FIGURE 2 As in Figure 1 except now for Na at 378 K.

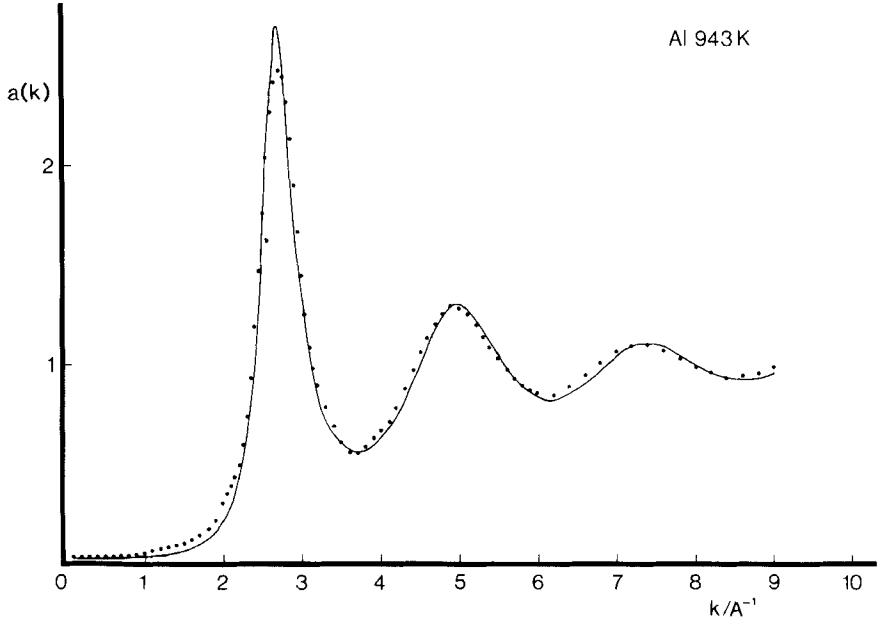

FIGURE 3 As in Figure 1 except now for Al at 943 K.

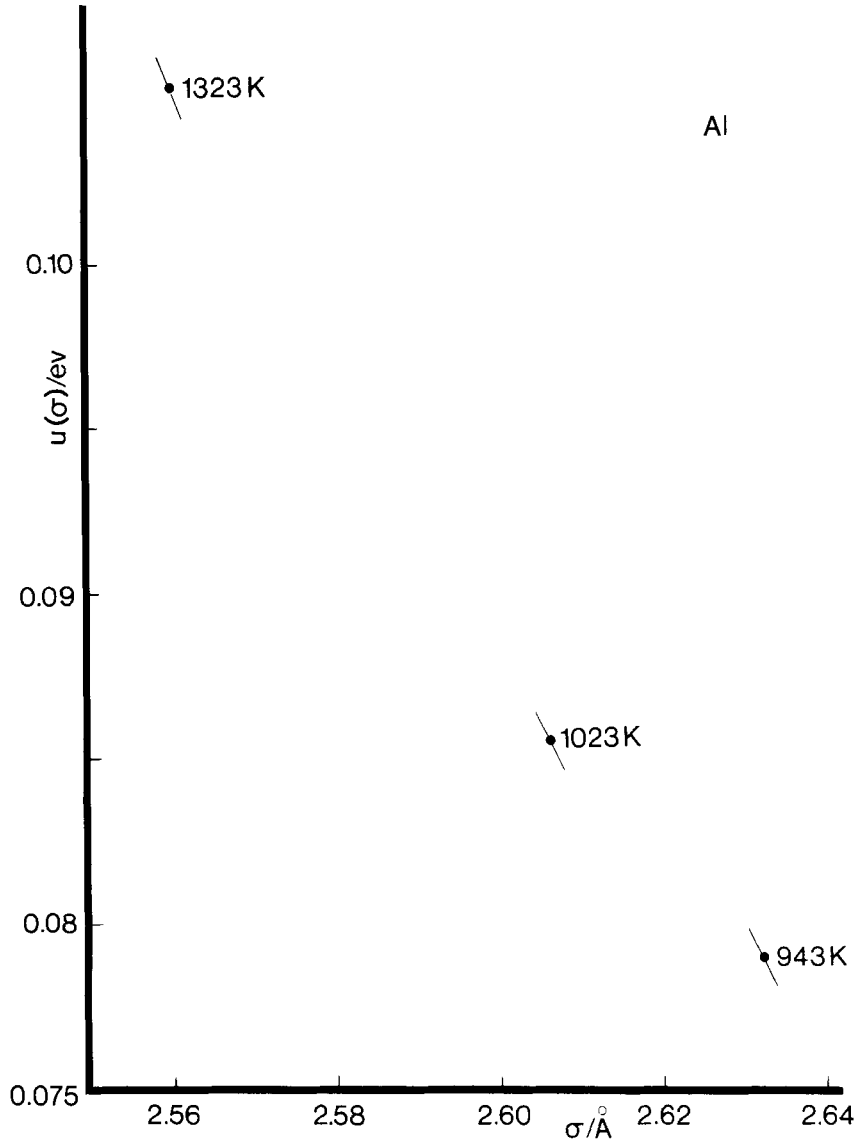

FIGURE 4 $u(\sigma)$, $u'(\sigma)$ versus σ for Al (data from Table I).

VI NOBLE METALS

Our fit for Ag at melting is shown in Figure 5. It is not as good as for Mg, Al and Pb (not to mention the inert gas liquids) but nevertheless the present theory is still clearly relevant.

We repeat the plot of Figure 4 except now for the Ag data of Table I and the result is shown in Figure 6. There is consistency for the three lowest temperatures but the diameter for the fourth is clearly suspect. Waseda states that his data for the latter case are less reliable than for the other three and this is in accord with our conclusion.

Similar analyses have been made for Cu and Au. The results (including confirmation of Waseda's assessment that the highest temperature data in each case are the least accurate) are very similar (see Table I).

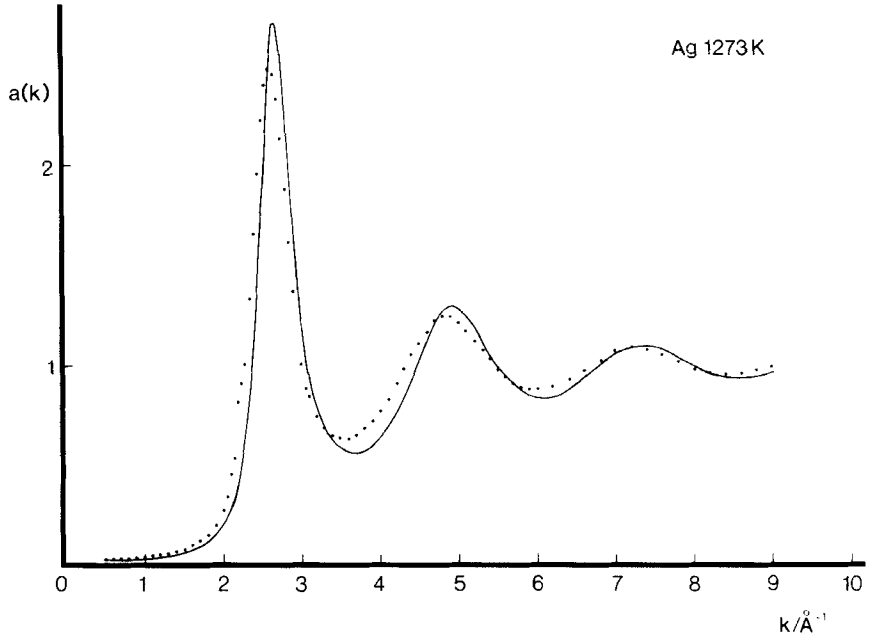

FIGURE 5 As in Figure 1 except now for Ag at 1273 K.

VII TRANSITION METALS

Here the structure factor fits are poorer than for the noble metals. Indeed the fits are very similar in character to those obtained for the alkalis, presumably because they are equally soft (in the sense of Table III). As an example, we show the case of Ni near melting in Figure 7 and this may be compared with that for Na in Figure 2.

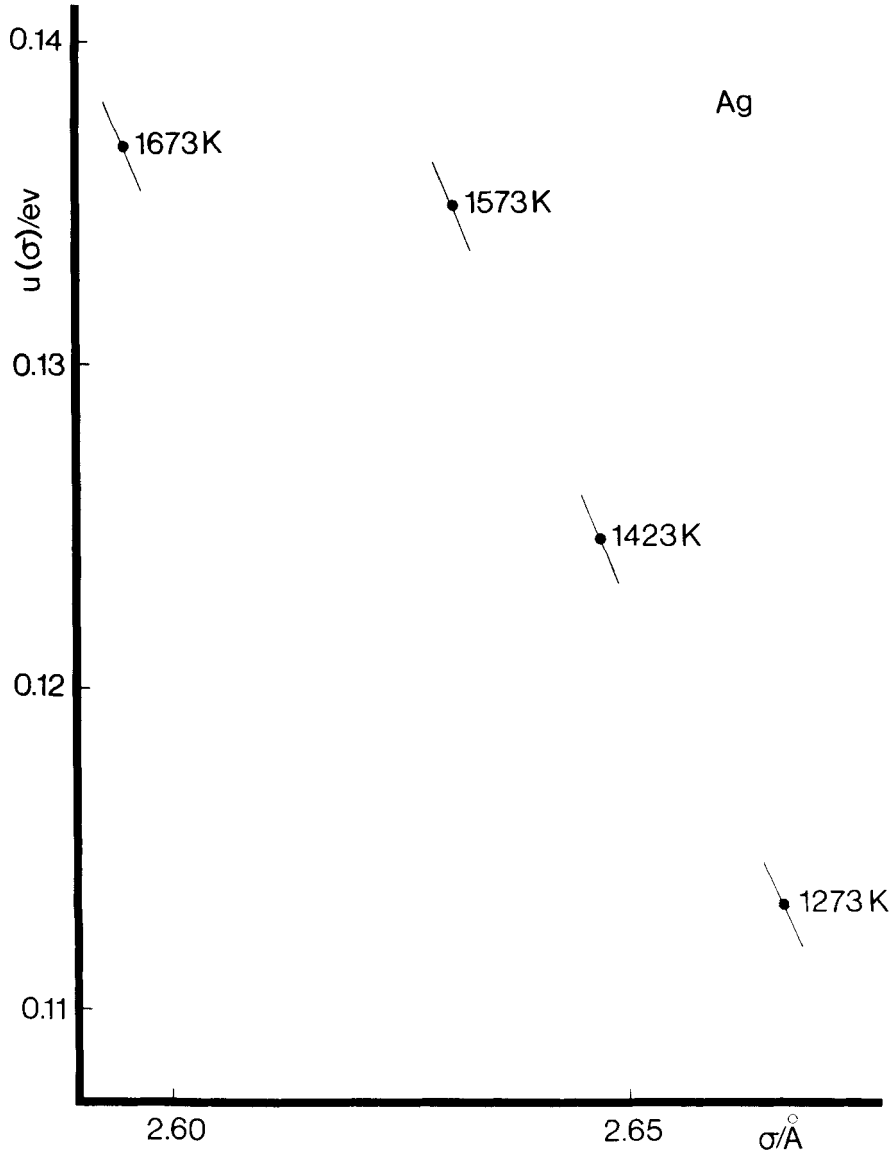

FIGURE 6 As in Figure 4 except now for Ag.

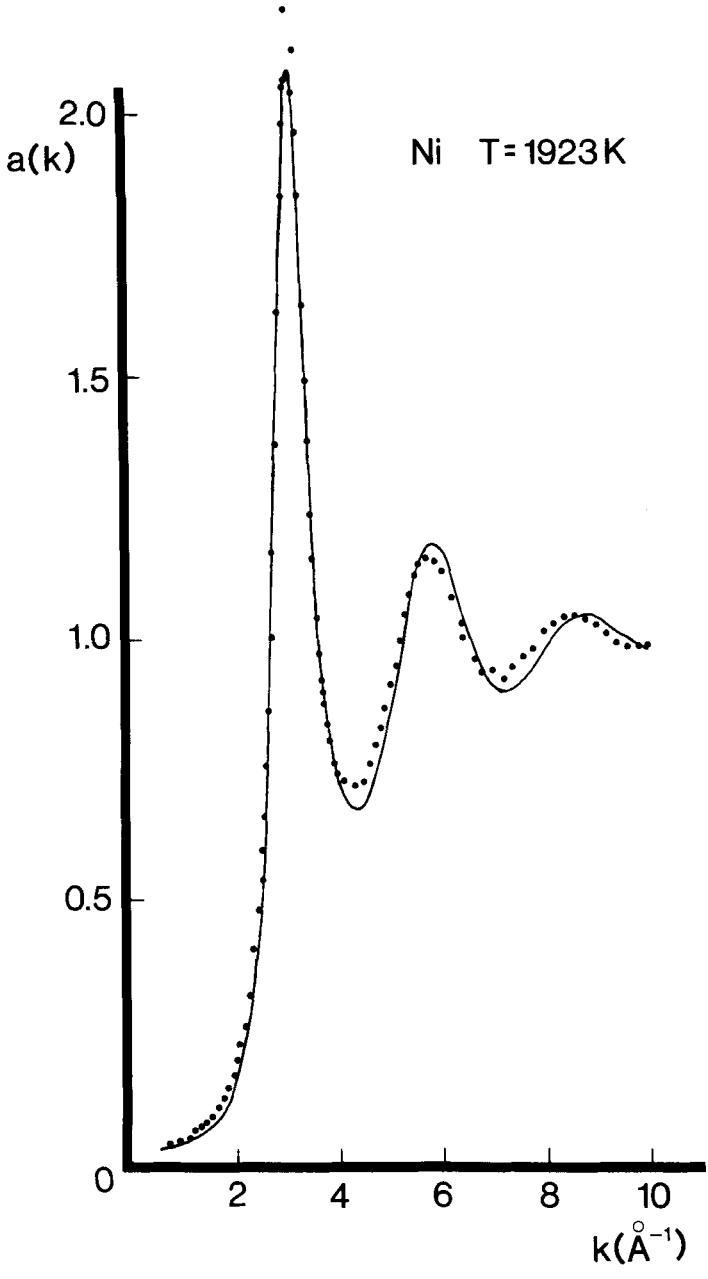

FIGURE 7 As in Figure 1 except now for Ni at 1923 K.

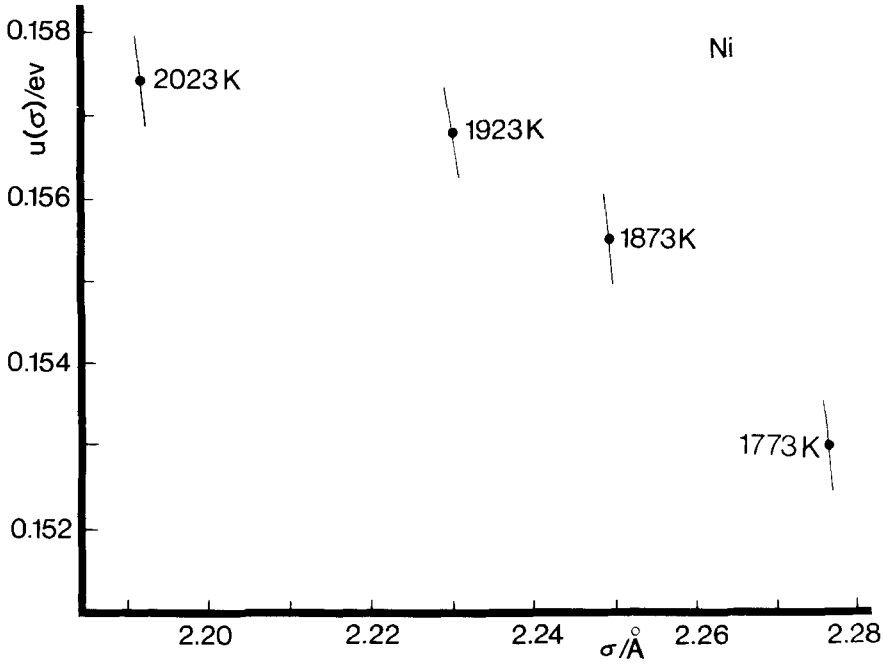

FIGURE 8 As in Figure 4 except now for Ni.

More disturbingly Figure 8 reveals, for Ni, values of $u'(\sigma)$ which are consistent with each other but not with the trend of $u(\sigma)$ versus σ. In the only other cases of transition metals where sufficient data are available, the results for Co do not show a smooth trend in $u(\sigma)$ versus σ while those for Fe are inconclusive. The behavior shown in Figure 8 is very similar to that exhibited by the entries for the two highest temperatures in Figure 6 and we attributed that to experimental error in the highest temperature case. It may therefore be that improved measurements at these very high temperatures will eliminate the inconsistency; we do not know. Because of the above problem, we have chosen to record in Table I only the result nearest melting for each transition metal.

Despite this unresolved worry, the results for the transition metals contain manifestly reasonable physical features. For example, we show in Figure 9 some core diameters. The values at the respective melting temperatures correlate moderately well with those obtained by a heuristic argument by Waseda, except that his value for Co is (we believe—see below) relatively too big and therefore out of sequence.

It is, perhaps, fairer to compare diameters at the same temperature. We do not have enough direct information to do this precisely but the following

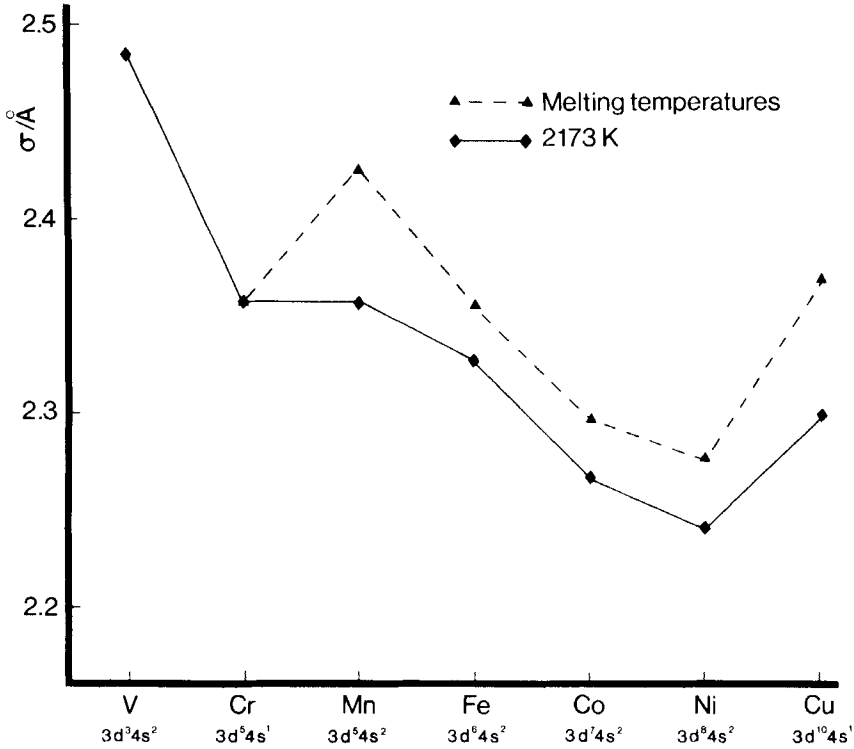

FIGURE 9 Diameters for transition metals at melting and at 2173 K. The atomic structure for the transition metals is Ti($3d^2 4s^2$), V($3d^3 4s^2$), Cr($3d^5 4s^1$), Mn($3d^5 4s^2$), Fe($3d^6 4s^2$), Co($3d^7 4s^2$), Ni($3d^8 4s^2$), Cu($3d^{10} 4s^1$).

procedure cannot be far wrong (and, indeed, as the reader may easily verify, works quite well for the temperature dependent data shown in Table I). Suppose we require a diameter $\sigma + \Delta\sigma$ at a temperature ΔT higher than that for which data σ and $-\sigma u'(\sigma)$ are available. We might expect an average kinetic energy[16] $\sim k_B \Delta T$ to be available in each collision and that this can be converted to potential energy to define a reduced effective diameter. Then approximating $u'(\sigma)$ by $k_B \Delta T/\sigma$ leads to $\sigma + \Delta\sigma = \sigma\{1 - k_B \Delta T/\sigma u'(\sigma)\}$. Results obtained in this way from the data of Table I are shown for 2173 K in Figure 9.[17]

This revised presentation removes the peaking at Mn shown in the melting point data and shows a physically plausible decrease in diameter as the transition series is traversed. The one case, Cr, where there is an irregularity probably itself reflects a physical fact when the anomalous *d*-shell filling in the atoms is borne in mind (Figure 9, caption).

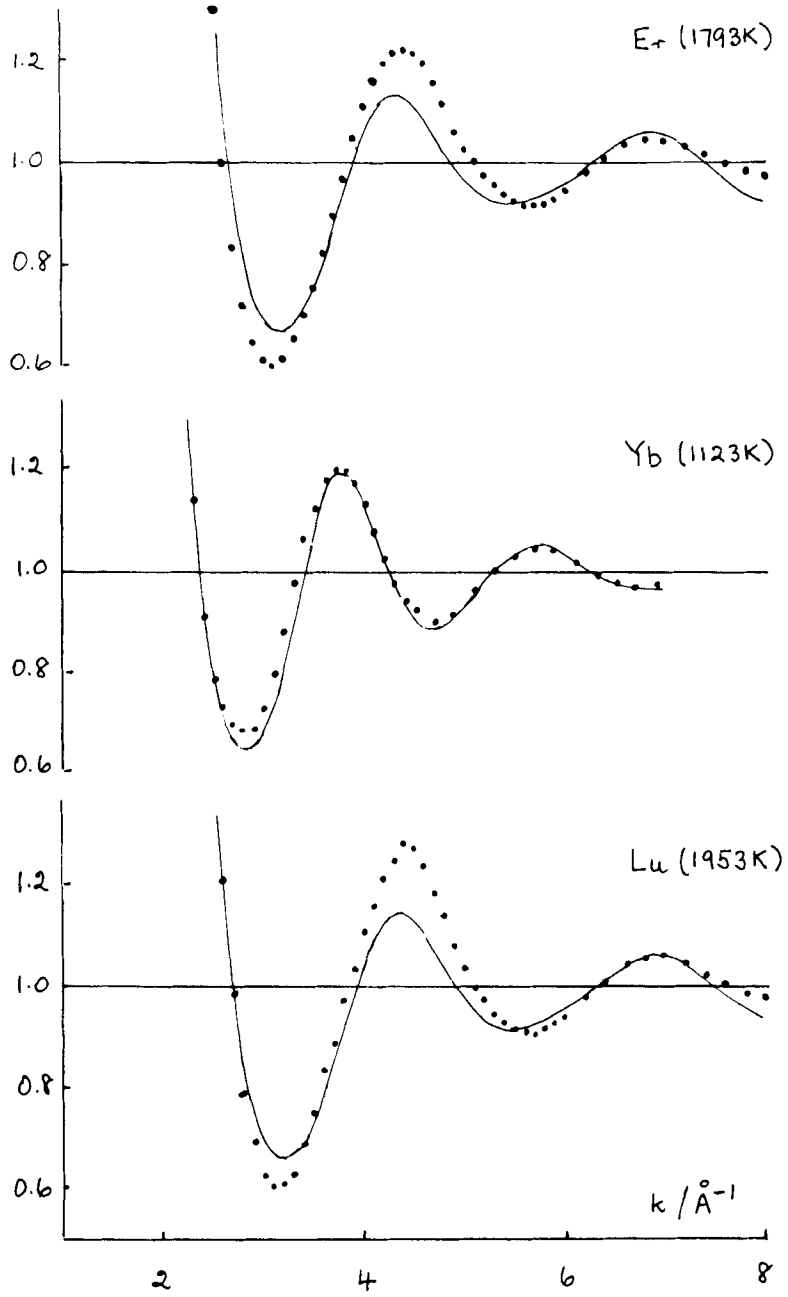

FIGURE 10 As in Figure 1 except now for Er. Yb and Lu.

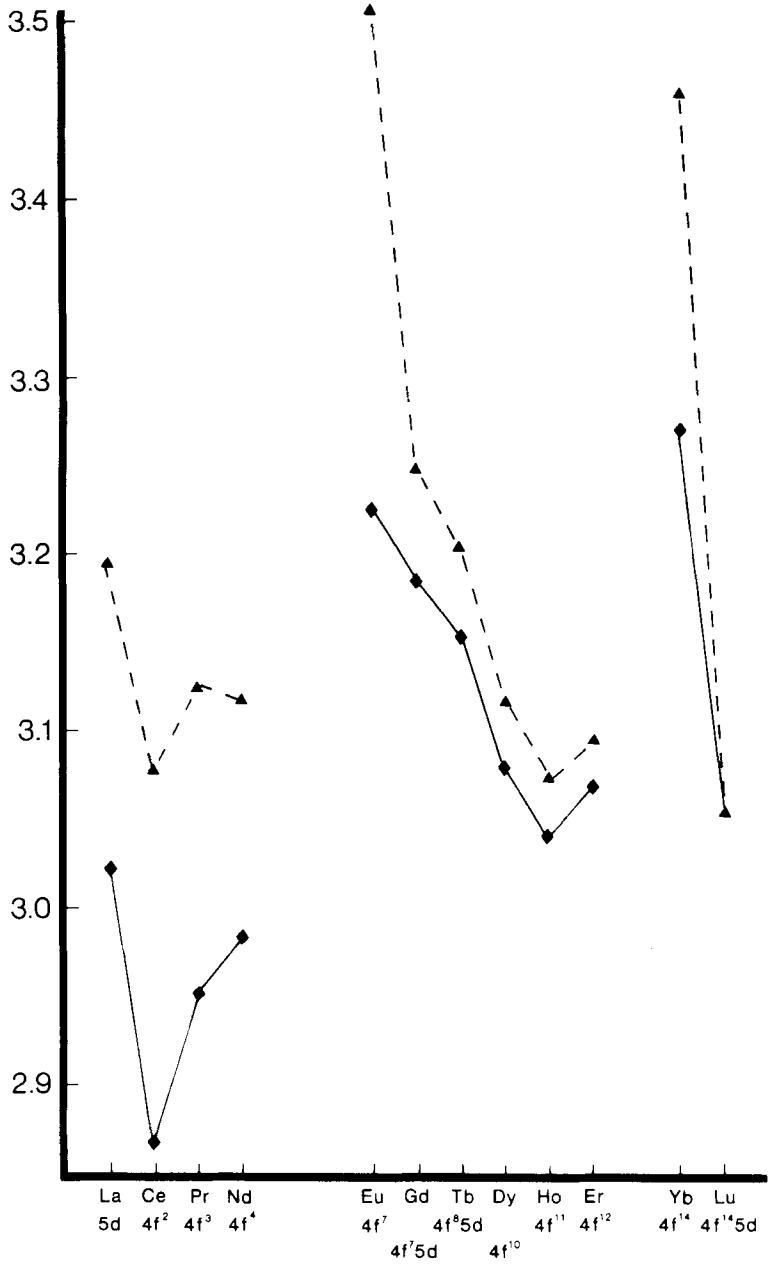

FIGURE 11. Diameters for lanthanides at melting and at 1953 K. The atomic structure for the lanthanides is La($5d6s^2$), Ce($4f^26s^2$), Pr($4f^36s^2$), Nd($4f^46s^2$), Pm($4f^56s^2$), Sm($4f^66s^2$), Eu($4f^76s^2$), Gd($4f^75d6s^2$), Tb($4f^85d6s^2$), Dy($4f^{10}6s^2$), Ho($4f^{11}6s^2$), Er($4f^{12}6s^2$), Tm($4f^{13}6s^2$), Yb($4f^{14}6s^2$), Lu($4f^{14}5d6s^2$).

VIII LANTHANIDES

The structure factor fits for the lanthanides are variable in their quality and we have not therefore explored further the limited available data on the temperature dependences of their structure factors. As illustrations, we quote in Figure 10 for a good case (Yb) in sequence between more typical examples. In the latter cases, we attribute the discrepancy at the highest k shown to an attempt to force an earlier fit (essentially between the third and fifth nodes) using a deficient parametrization.

Notwithstanding the above comments, we used our results (Table I) to examine the diameter variation across the lanthanide series and the results are shown in Figure 11. To obtain the data at constant temperature, we used precisely the method explained in the previous section when obtaining Figure 9 for the transition metals.

In contrast with the transition metals, Hund's rule filling appears to operate in some sense in deciding the relative sizes of the diameters, these increasing (at constant temperature) from Ce to Eu and then decreasing to Ho. On this basis, we might have expected further shrinkage to have been observed in Er and perhaps it is relevant to note that Waseda states that of his lanthanide measurements, he expects those for Er and Lu to be the least accurate.

At a cruder level, we can say the lanthanide diameters are all much the same (a little over 3 Å). There is, however, a variation in the core hardnesses which, as Table III shows, becomes greater as one proceeds from the lighter to the heavier elements. The increased hardness can thus be plausibly ascribed to the unfavourable energetics of pseudoatom overlap when the f orbitals become doubly filled by a process akin to Hund's rule for atoms. These observations more or less agree with the conclusions reached by Waseda and Tamaki[18] (see also Waseda[1]) in a more qualitative study.

Finally, it is worth remarking that Table I shows that at melting the lanthanides have the smallest packing fraction of all the metals, a point also noted by Waseda[1]. Instead of the usual values ~ 0.5, reduced values of ~ 0.45 are obtained. In addition, as we have seen (Table III) they have the softest cores (in the sense of Section III) of all the cases we have studied.

IX CONCLUSIONS

We have suggested that limited but physically revealing information (especially effective collision diameters σ and associated forces $-u'(\sigma)$) can be extracted from the large argument parts of the currently available liquid structure factors. Our procedure amounts to the inversion of that of WCA so that the physical assumptions of that theory are implicit in the present work. In particular, we assume that the free energy and the part of the structure

factor under study are core dominated. This would appear to be a reasonable hypothesis for inert gas and simple and noble metal liquids, and the quality of structure factor fit and the internal consistency checks (detailed in Sections IV, V and VI) tend to confirm this.

The situation is less clear for transition metals and the rare earths. Nevertheless, as we have seen, some plausible and interesting trends can be extracted from the data.

Acknowledgement

We are grateful for the support of the U.K. Science and Engineering Research Council.

References

1. Y. Waseda, *The Structure of Non-Crystalline Metals*, McGraw-Hill (New York, 1980).
2. J. D. Weeks, D. Chandler and H. C. Andersen, *J. Chem. Phys.* **54**, 5237 (1971); H. C. Andersen, D. Chandler and J. D. Weeks, *Advan. Chem. Phys.* **34**, 105 (1976).
3. Ref. 2; also, for the modified formalism of this paper, see R. Jacobs and H. C. Andersen, *Chem. Phys.* **10**, 73 (1975).
4. A. Meyer, M. Silbert and W. H. Young, *Chem. Phys.* **49**, 147 (1980).
5. Some liquid metals exhibit first peak anomalies (Ref. 1) which may, in turn, reflect anomalous core behavior (M. Silbert and W. H. Young, *Phys. Lett.* **58***A*, 469 (1976); K. K. Mon, N. W. Ashcroft and G. V. Chester, *Phys. Rev.* **B19**, 5103 (1979). Since the WCA method is designed (Section III) to cope only with smoothly monotonic core potentials, such systems have been excluded from our study.
6. A letter (A. Meyer, M. Silbert and W. H. Young, *Phys. Chem. Liq.* **10**, 279 (1981)) has already appeared and we presented a paper at the recent LAM5 Los Angeles Conference in which the data for Pb from several sources were thus analysed.
7. R. E. Jacobs and H. C. Andersen, *Chem. Phys.* **10**, 73 (1975). This eliminates a spurious bump at low k in the WCA structure factor. Although the low k behavior is of no direct interest for present purposes, the correction has small quantitative implications for high k, as Ref. 4 demonstrates.
8. $a(k)$ and $g(r)$ are given by the work of E. Thiele, *J. Chem. Phys.* **39**, 474 (1963) and M. S. Wertheim, *Phys. Rev. Lett.* **10**, 321 (1963). Using the Appendix of Ref. 4, one may then readily verify that

$$Y = -(1 - \eta)(2 + \eta)/9(1 + \eta) \quad \text{and} \quad \mu = 72\eta(1 + \eta)(2 + \eta)/(1 - \eta)^2(16 + 9\eta + \eta^2).$$

9. L. Verlet and J-J. Weis, *Phys. Rev.* **A5**, 939 (1972).
10. J. L. Yarnell, M. J. Katz, R. G. Wenzel and S. H. Koenig, *Phys. Rev.* **A7**, 2130 (1973).
11. L. A. de Graaf and B. Mozer, *J. Chem. Phys.* **55**, 4967 (1971).
12. N. W. Ashcroft and D. C. Langreth, *Phys. Rev.* **156**, 685 (1967).
13. M. Silbert and W. H. Young, *J. Phys.* **C14**, 2425 (1981).
14. The fit is significantly poorer than for Ni (Figure 7) and Eu (Figure 9).
15. In principle, these potentials are density dependent so we are really sampling different curves at different temperatures and, in particular, the tangents $u'(\sigma)$ will not precisely give the slope of $u(\sigma)$ versus (σ). But the effect is probably insignificant because of the small density variations involved and, in practice, is swamped by the larger experimental errors which we believe to be principally responsible for the random features of Figures 4 and 6.
16. This argument is the same as that of Ref. 12 except here we use $k_B\Delta T$ rather than $\frac{3}{2}$ of this value in view of our comments in Section III.
17. If we discount the highest temperature case shown in Figure 8, the different answers obtainable from those data for Ni at 2173 K do not vary sufficiently to suggest to us that the general trend shown in Figure 9 can be thus prejudiced.
18. Y. Waseda and S. Tamaki, *Phil. Mag.* **32**, 273 (1975); *J. Phys.* **F7**, L151 (1977).